

BINARY EVENTS AND EXTRAGALACTIC PLANETS IN PIXEL MICROLENSING

EDWARD A. BALTZ

ISCAP, Columbia Astrophysics Laboratory, 550 W 120th St., Mail Code 5247, New York, NY 10027

AND

PAOLO GONDOLO

Department of Physics, Case Western Reserve University, 10900 Euclid Ave., Cleveland, OH 44106-7079

Draft version August 16, 2018

ABSTRACT

Pixel microlensing, i.e. gravitational microlensing of unresolved stars, can be used to explore distant stellar systems, and as a bonus may be able to detect extragalactic planets. In these studies, binary-lens events with multiple high-magnification peaks are crucial. Considering only those events which exhibit caustic crossings, we estimate the fraction of binary events in several example pixel microlensing surveys and compare them to the fraction of binary events in a classical survey with resolved stars. We find a considerable enhancement of the relative rate of binary events in pixel microlensing surveys, relative to surveys with resolved sources. We calculate the rate distribution of binary events with respect to the time between caustic crossings. We consider possible surveys of M31 with ground-based telescopes and of M87 with HST and NGST. For the latter, a pixel microlensing survey taking one image a day may observe of order one dozen binary events per month.

Subject headings: binaries:general — gravitational lensing — planetary systems

1. INTRODUCTION

Gravitational microlensing has been a powerful probe of massive dark objects in the galactic halo (Paczynski 1986; Griest 1991; Alcock et al. 1995). If the lens is a binary, a pair of caustic crossings may be observed. The caustics of the lens system are curves on which the magnification is formally infinite, and quite large in practice. In addition to caustic crossing events, binary lenses can give smaller perturbations to a standard microlensing lightcurve. Such perturbations are in principle detectable (Mao & di Stefano 1995; di Stefano & Perna 1997). Binary events yield more information about the source–lens system than single–lens events, and it is even possible to image the surface of the source star due to the large magnification. Caustic crossing events have been seen towards the galactic bulge and the Small and Large Magellanic Clouds (Alcock et al. 1997; 2000a; Afonso et al. 1998; Albrow et al. 1995; 1999; Udalski et al. 2000; Afonso et al. 2000). Mao & Paczynski (1991) studied caustic crossing events in classical microlensing. They came to the conclusion that approximately 7% of microlensing events towards the galactic bulge would exhibit caustic crossings, with the assumption of perfect time sampling.

The pixel technique extends the feasibility of microlensing experiments by removing the requirement that individual stars be resolved (Crotts 1992, Baillon et al. 1993). The possibility of detecting caustic crossings due to binary lenses in pixel events is intriguing, as it allows us to study stellar populations at great distances. Several groups have successfully used the pixel, or difference image analysis technique to detect candidate microlensing events towards M31 (Crotts & Tomaney 1996; Ansari et al. 1999). The MACHO collaboration has also used this technique to identify candidates towards the LMC, in addition to the classical events (Alcock et al. 1999). This

technique has a great future as more telescope resources are brought to bear, both on the ground and in space. Space based surveys will allow the reach of microlensing surveys to extend at least as far as the Virgo cluster, at a distance of about 16 Mpc.

In this paper, we extend the Mao & Paczynski (1991) analysis to pixel microlensing surveys of stellar systems. In pixel microlensing, detected single–lens events tend to have high magnifications, so their rate is suppressed by a factor of $1/A$, where A is the magnification required for detection. However, caustic crossing events always exhibit large magnifications at the caustic crossings. This enhances the rate of caustic crossing events relative to single–lens events in pixel microlensing. On the other hand, finite source effects will limit the maximum magnification during a caustic crossing, rendering some classically detectable caustic crossing events undetectable in pixel microlensing. In this paper we show that the larger region of high magnification is the stronger effect. As a result, caustic crossing events in pixel microlensing represent fractions of 10–15% of microlensing events, compared with the 2–3% fraction we find for observable caustic crossing events with resolved sources. Finer time sampling would increase both fractions, and the latter would then agree with the Mao & Paczynski (1991) result.

Our primary goal with this work is to show that microlensing events exhibiting caustic crossings are detectable in pixel microlensing surveys. To this end, we estimate the rate of caustic crossing events given some basic assumptions. Less important to our purposes are considerations of accurately determining the properties of the source–lens system, which we leave to future work.

2. THE TWO POINT MASS GRAVITATIONAL LENS

We begin with a theoretical discussion of the two point mass gravitational lens, the appropriate model of a binary star system. This model has been studied extensively (Schneider & Weiß 1986; Erdl & Schneider 1993). We quote some relevant results. We take the masses of the lenses to be M_1 and M_2 , with $M = M_1 + M_2$, and we define dimensionless masses $\mu_{1,2} = M_{1,2}/M$ such that $\mu_1 + \mu_2 = 1$. Furthermore, we define $q = M_2/M_1$, with $0 \leq q \leq 1$ without loss of generality. We take the standard notation of distances to the source $D_s = L$, deflector $D_d = xL$, and deflector–source distance $D_{ds} = (1-x)L$. We define the Einstein radius and the Einstein angle for the system as (Einstein 1936)

$$R_E = \sqrt{\frac{4GML}{c^2}x(1-x)}, \quad \theta_E = \frac{R_E}{Lx}. \quad (1)$$

We adopt a complex parameterization (Witt 1990) of the lens system. We introduce complex angular coordinates on the plane of the sky, $z = (\theta_x + i\theta_y)/\theta_E$. Given two lenses at angular positions z_1 and z_2 , a source at ζ will have images at the solutions z of the lens equation

$$\zeta = z - \frac{\overline{\alpha(z)}}{\alpha(z)} = z - \frac{\mu_1}{\bar{z} - \bar{z}_1} - \frac{\mu_2}{\bar{z} - \bar{z}_2}. \quad (2)$$

Here α is the deflection angle, and the bars indicate complex conjugation. We will call the plane described by ζ the source plane, and the plane described by z the image plane. The variables ζ and z are angles expressed in units of the Einstein angle θ_E . A source at angular position ζ is at a transverse distance $L\theta_E|\zeta| = R_E|\zeta|/x$ from the line of sight through the origin of the coordinate system. Likewise, a lens at angular position z is at a distance $xL\theta_E|z| = R_E|z|$ from the line of sight through the origin. We are interested in the *apparent* physical size of the caustic curves, as this determines the allowed *physical* trajectories of the source which produce caustic crossings. The caustic curve, when considered to be in the physical source plane, is given by $L\theta_E\zeta = R_E\zeta/x$.

In this formalism, the Jacobian of $\zeta(z)$ in eq. (2) is

$$J(z) = 1 - \left| \frac{\partial \alpha}{\partial z} \right|^2. \quad (3)$$

The magnification of an image at z is given by $1/|J(z)|$, with the sign of $J(z)$ giving the parity of the image. The total magnification is the sum of the individual magnifications of the images.

The points z where the Jacobian vanishes, $J(z) = 0$, trace out the critical curves. The inverse images $\zeta(z)$ of the critical curves are the caustic curves. When the source is on a caustic, and so its images are on the critical curve, the magnification is formally infinite.

Let d be the angular distance between the two lenses in units of the Einstein angle θ_E . According to the value of d , there are three regimes in a binary lens system: the so-called close, intermediate, and wide binaries. A close binary exhibits three caustics, one with four cusps on the line of the lenses and two with three cusps off the line. The intermediate binary exhibits one six-cusped caustic, and the wide binary exhibits two four-cusped caustics on the

lens line. The separation points d_{CI} and d_{IW} between close and intermediate and between intermediate and wide binaries are as follows (Erdl & Schneider 1993; Rhie & Bennett 1999),

$$d_{\text{IW}} = \left(\mu_1^{1/3} + \mu_2^{1/3} \right)^{3/2}, \quad d_{\text{CI}} = \frac{1}{\sqrt{d_{\text{IW}}}}. \quad (4)$$

In the equal mass case, $\mu_1 = \mu_2 = 1/2$, we have $d_{\text{IW}} = 2$ and $d_{\text{CI}} = 1/\sqrt{2}$. As $\mu_1\mu_2 \rightarrow 0$, the intermediate binary vanishes, and the transition between close and wide is at $d_{\text{CI}} = d_{\text{IW}} = 1$.

The critical curves are simply parameterized by (Witt 1990)

$$e^{-i\phi} = -\frac{\partial \alpha}{\partial z}. \quad (5)$$

At each ϕ , there are four roots of the resulting quartic equation in z . Each root $z_i(\phi)$ ($i = 1, \dots, 4$) describes a portion of the critical curve. Extending the parameter range to $0 < \phi < 8\pi$, these portions can be patched together so that they follow each other continuously for every disjoint piece of the caustic. In this way, we achieve one “continuous” parameterization of the caustic, $z = z(\phi)$. The continuous parameterization is explicitly given by

$$z(\phi) = \frac{1}{2} \left[-\tilde{\sigma} + e^{i\phi/2} \sqrt{e^{-i\phi} \left(-2a - \tilde{\sigma}^2 + \frac{2b}{\tilde{\sigma}} \right)} \right], \quad (6)$$

with

$$\tilde{\sigma} = e^{i\phi/4} \sqrt{e^{-i\phi/2} \sigma^2}, \quad (7)$$

$$\sigma = \sqrt{-2a/3 + u_+ + u_-}, \quad (8)$$

$$a = -\left(\frac{d^2}{2} + e^{i\phi} \right), \quad (9)$$

$$b = -d\mu e^{i\phi}, \quad (10)$$

$$\mu = \mu_1 - \mu_2, \quad (11)$$

$$u_{\pm} = \sqrt[3]{r \pm \sqrt{s^3 + r^2}}, \quad (12)$$

$$s = -\left(\frac{d^2 - e^{i\phi}}{3} \right)^2, \quad (13)$$

$$r = \left(\frac{d^2 - e^{i\phi}}{3} \right)^3 + \frac{1}{2} d^2 e^{2i\phi} (\mu^2 - 1). \quad (14)$$

Here, μ gives the degree of asymmetry of the lens, b is something like a dipole moment about the origin, and the other parameters have no obvious simple interpretation. The parameterization of the caustics, $\zeta = \zeta(\phi)$, follows trivially from that of the critical curves, $z = z(\phi)$, using the lens equation, eq. (2).

Lastly, we expand the parameterizations of the critical curves and caustics in the limits where $d \rightarrow 0, \infty$. Defining $u = \exp(i\phi/2)$ with $0 < \phi < 4\pi$, we find as $d \ll d_{\text{CI}}$:

$$z \approx u + \frac{1}{2}\mu d + \frac{3(1-\mu^2)}{8u}d^2, \quad (15)$$

$$\zeta \approx \frac{1}{2}\mu d + \frac{(1-\mu^2)}{8} \frac{3+u^4}{u} d^2, \quad (16)$$

with $O(d^3)$ errors and as $d \gg d_{1W}$:

$$z \approx \frac{1}{2}d + u\sqrt{\frac{1+\mu}{2}} \left(1 + \frac{(1-\mu)u^2}{4d^2}\right), \quad (17)$$

$$\zeta \approx \frac{1}{2}d - \frac{1-\mu}{2d} \left(1 - \sqrt{\frac{1+\mu}{2}} \frac{3+u^4}{2ud}\right), \quad (18)$$

with $O(d^{-3})$ errors.

3. RATE OF CAUSTIC CROSSING

In computing the rate of single-lens events, the Einstein angle is used as a “cross section” for microlensing. Any source which passes inside the Einstein ring is said to be microlensed. Griest (1991) has shown that the rate of single-lens events depends linearly on the threshold minimum angular separation between source and lens, implying that the dependence is on the angular diameter rather than on the solid angle, which would imply a quadratic dependence on the impact parameter. In contrast, the optical depth is a measure of the probability that a given star is microlensed at a given instant. This is proportional to the area of the Einstein ring.

To compute the rate of caustic crossing events, we compute the “angular diameter” of the caustic structure in direct analogy to the single-lens case. We will call it the “angular width” of the caustic. We will appropriately average this “angular width” over the distribution of binary systems. The optical depth to caustic crossing would similarly depend on the solid angle enclosed by the caustic, but the rate of caustic crossing events depends on the angular width, as we now show.

In a caustic crossing event, the source crosses the caustic an even number of times, half entering and half exiting the interior of the caustic. Consider the rate Γ_0 at which the sources enter the region limited by the caustic. The number of caustic crossings per unit time, counting each caustic peak in the lightcurve, is then $2\Gamma_0$. If the orientation of the caustic is random, as is the case for binary systems whose separation has no preferred direction in the sky, we find

$$\Gamma_0 = \Phi w, \quad (19)$$

where Φ is the angle-averaged number flux of the sources, and w is the “width of the caustic,” defined in terms of the caustic length ℓ by

$$w = \frac{\ell}{\pi}. \quad (20)$$

We take w and ℓ in units of θ_E , and Φ in the corresponding units.

Eqs. (19) and (20) are proven as follows. The flux of sources whose proper motion is in a direction forming an angle ψ with the binary separation is $\Phi d\psi/(2\pi)$. Consider an infinitesimal piece of the caustic $d\ell$, whose interior normal makes an angle θ with the fixed axis. The number of sources entering the caustic through $d\ell$ per unit time is

$$d\Gamma_0 = \int_{\theta-\frac{\pi}{2}}^{\theta+\frac{\pi}{2}} \frac{d\psi}{2\pi} \Phi \cos(\psi - \theta) d\ell = \Phi \frac{d\ell}{\pi} = \Phi dw. \quad (21)$$

The limits of integration restrict the flow of sources to those coming from one side of the caustic only. Integration of eq. (21) along the caustic gives eqs. (19) and (20).

Eqs. (19) and (20) apply to any closed curve in the plane. For example, consider the rate of single lens events. The critical curve of a single lens is a circle, namely the Einstein ring. Its circumference is its length ℓ , and eq. (20) implies that w is the diameter of the circle. Then eq. (19) states the obvious fact that the number of sources entering the circle equals the flux times the circle diameter.

This method of computing the cross section of a closed curve counts all entries to the curve. A curve that is not convex, such as a caustic curve, can have multiple entries. The rate Γ_0 counts all of these entries. For example, a binary lens event with 4 caustic crossings is counted twice in Γ_0 . In other words, the rate Γ_0 is half the number of caustic peaks per unit time.

4. BINARY SYSTEMS

We now discuss the observed physical parameters of binary systems relevant to our calculation. It is well known that a large fraction of stars have companions, perhaps the majority. A well-known rule of thumb is that the distribution of periods P for binary systems is constant in $\ln P$, with roughly 10% of binaries in each decade from one-third day to ten million years. Less well known is the correlation between the masses of the bound stars. At high masses, a correlation is seen, but at low masses, the data are inconclusive.

We proceed to express the separation of the binary pair in terms of its period and total mass. With semimajor axis a , Kepler’s law reads

$$\left(\frac{a}{\text{AU}}\right)^3 = \left(\frac{M}{M_\odot}\right) \left(\frac{P}{\text{yr}}\right)^2. \quad (22)$$

The Einstein radius is

$$\left(\frac{R_E}{\text{AU}}\right) = B \sqrt{\frac{M}{M_\odot}}, \quad (23)$$

with $B = 0.28538 \sqrt{x(1-x)} 10^{D/10}$, and D is the distance modulus to the source. Assuming that the projected separation is at maximum, the most probable situation, we find the relation

$$d = \left(\frac{2}{B}\right) \left(\frac{P}{\text{yr}}\right)^{2/3} \left(\frac{M}{M_\odot}\right)^{-1/6}. \quad (24)$$

In the range $P/\text{yr} = [10^{-3}, 10^7]$, the distribution in P is simply $dN/d \log P = 1/10$, and is correctly normalized. Fixing all other quantities, appropriate for the rate calculation we will do, we thus find the distribution of binaries in d , $dN/d \log d = 3/20$.

There is disagreement about the distribution in q of binary systems, ranging from a linear rise $\propto 2.6 + 2.9q$ (Mazeh et al. 1992) to a power law decline $\propto q^{-1.3}$ (Patience et al. 1998), with other measurements falling between (Duquenooy & Mayor 1991; Trimble 1990). In the next section we will find that the effects of the q distribution of binaries are mild.

5. SIZE OF CAUSTIC STRUCTURE

We evaluate the mean width of the caustics w for the binary systems described in the previous section. In the parametric representation of the caustic $\zeta = \zeta(\phi)$, its length in units of the Einstein angle is

$$\ell = \int_0^{8\pi} \left| \frac{d\zeta}{d\phi} \right| d\phi = 2 \int_0^{8\pi} \left| \operatorname{Re} \left(e^{-i\phi/2} \frac{dz}{d\phi} \right) \right| d\phi. \quad (25)$$

We have computed the length of the caustic structure for various values of q . The caustic length is not as sensitive to the q distribution as it is to the lens separation d , as we show in figure 1. There we plot the width of the caustic as a function of d , averaging over four distributions in q : a linear rise $\propto 2.6 + 2.9q$, flat, flat in $\ln q$, and a power law $q^{-1.3}$ (in the last two distributions we take $q > 0.1$). The difference is only a few per cent. The peaks occur at the average values of the close–intermediate and intermediate–wide binary separations d_{CI} and d_{IW} .

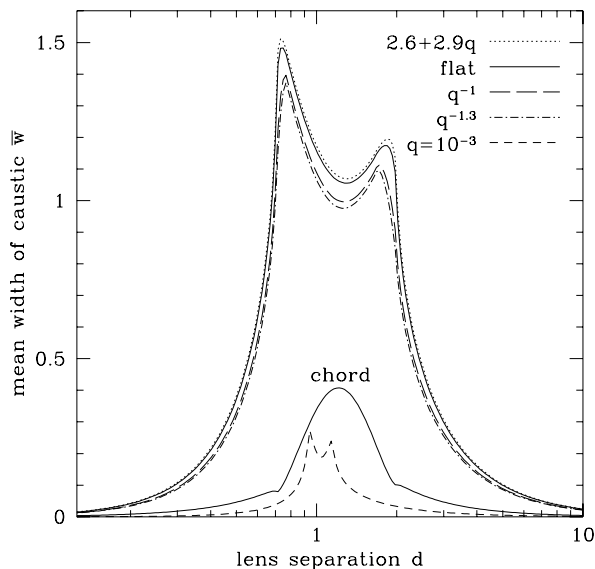


FIG 1.— Average width w of caustic structure as a function of lens separation d , both in units of the Einstein angle θ_E . We have averaged over several distributions in the binary mass ratio q , and also included the case $q = 10^{-3}$, of interest for planetary binaries. We have also plotted the mean chord length, averaged over the flat q distribution.

For small and large separations d , we have found the leading behavior of the mean caustic width. In both cases the important caustics are approximately square. For $d < d_{\text{CI}}$, the linear dimension of the two additional triangular caustics is suppressed relative to the single, central square caustic by a factor of d . The mean width is $w = 3d^2(1 - \mu^2)/\pi$ in the case $d \ll d_{\text{CI}}$, and it is $w = 6(1 - \mu)\sqrt{2(1 + \mu)}/(\pi d^2)$ when $d \gg d_{\text{IW}}$. Thus, we see that the caustic structure is largest when d is of order unity. Averaging over the four q distributions mentioned above (namely $2.6 + 2.9q$, flat, $1/q$, and $q^{-1.3}$, in this order) we find $w/d^2 = 0.78, 0.74, 0.68$, and 0.64 in the case $d \ll d_{\text{CI}}$, and $wd^2 = 2.0, 1.85, 1.63$, and 1.51 in the case $d \gg d_{\text{IW}}$.

Now that we have computed the cross section for caustic crossing events, we can compare with that of single–lens

events on resolved stars, whose cross section in Einstein units is 2. The cross section averaged over angles is ℓ/π , which needs to be averaged over d and q . We find the ratio of caustic crossing to single–lens events to be approximately 6.3%, multiplied by the fraction of star systems that are binaries. This is in quite good agreement with the results of Mao and Paczyński (1991).

In addition to the mean width of the caustic structure, important for determining the cross section for caustic crossing events, we would like to know the mean length of chords through the caustic structure. This quantity is directly related to the mean time between caustic crossings. We proceed as follows. Let $w(\theta)$ be the projected width of the caustic structure at a fixed orientation θ , and let $C(\theta, b)$ be the chord length at orientation θ and impact parameter b . The area of the caustic structure is clearly

$$A = \int_0^{w(\theta)} db C(\theta, b) = w(\theta)C(\theta), \quad (26)$$

where now $C(\theta)$ is the mean chord length at orientation θ . The area is of course independent of θ . We want the mean chord length, weighted by the width of the caustic. The mean chord length over all orientations is now just

$$C = A \int_0^\pi \frac{d\theta}{\pi} \frac{1}{w(\theta)} \frac{w(\theta)}{\langle w \rangle} = \frac{A}{\langle w \rangle} = \frac{A\pi}{\ell}, \quad (27)$$

the area divided by the mean cross section. Note that on the occasions where there are multiple pairs of caustic crossings, the chord is counted as multiple separate pieces.

We will need the area and projected diameter of the caustic structure. In vector notation, we have $dA = (\vec{r} \times d\vec{r})/2$, which is easily transformed to the complex parameterization,

$$\begin{aligned} A &= \frac{1}{2} \left| \int_0^{8\pi} \operatorname{Im} \left(\bar{\zeta} \frac{d\zeta}{d\phi} \right) d\phi \right| \\ &= \left| \int_0^{8\pi} \operatorname{Im} \left(e^{-i\phi/2} \zeta \right) \operatorname{Re} \left(e^{-i\phi/2} \frac{dz}{d\phi} \right) d\phi \right|. \end{aligned} \quad (28)$$

The projected diameter along the real axis, at orientation θ , is simply

$$\begin{aligned} w(\theta) &= \frac{1}{2} \int \left| d \operatorname{Re}(e^{i\theta} \zeta) \right| \\ &= \frac{1}{4} \int_0^{8\pi} \left| e^{i\theta} \frac{d\zeta}{d\phi} + e^{-i\theta} \frac{d\bar{\zeta}}{d\phi} \right| d\phi \\ &= \int_0^{8\pi} \left| \cos \left(\theta + \frac{\phi}{2} \right) \operatorname{Re} \left(e^{-i\phi/2} \frac{dz}{d\phi} \right) \right| d\phi. \end{aligned} \quad (29)$$

Note that if this expression is averaged over orientations θ , we recover the result for the mean width of the caustic structure being proportional to the length of the caustic.

We have now assembled all of the necessary pieces for calculating the mean length of chords through the caustic curves. As for the mean diameter, we compute this quantity as a function of the lens spacing d , averaging over a distribution in q , which we take to be constant in q . The mean chord length is plotted in figure 1.

We are furthermore interested in the full distribution of chord lengths for a given lens configuration. As is done by Han, Park & Lee (2000), we have performed a Monte Carlo simulation to find this distribution. The results are shown in figure 2, with the exact mean shown as a short dashed line and the median shown as a long dashed line. From this simulation, it seems that using the mean chord length may not be an adequate prescription for designing a microlensing survey, since the distribution of chord lengths is quite complicated. However, we will find that the mean chord length prescription is usually quite good.

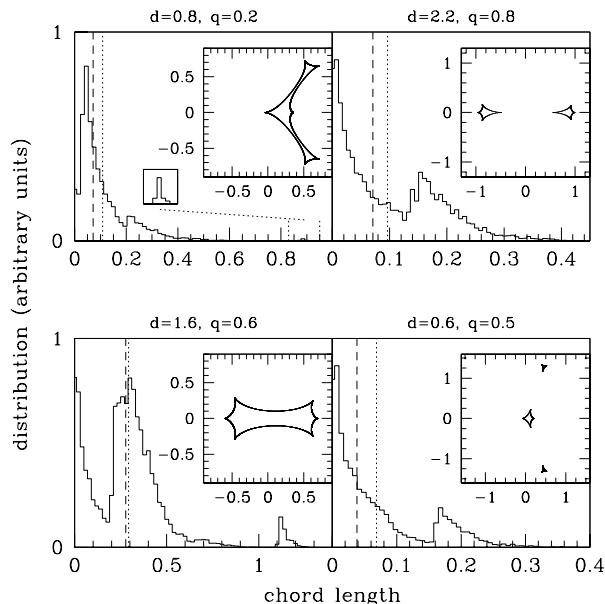


FIG 2.— Distributions of chord lengths for several choices of d and q . The exact means of these distributions are indicated by the short dashed lines, while the medians are shown by the long dashed lines. The small panels show the shapes of the caustic curves, with the masses at $x = \pm d/2$ and the larger mass on the right. The y-axis is in arbitrary units.

6. LIGHTCURVES AND FINITE SIZE EFFECTS

We illustrate two lightcurves for caustic crossing events in figure 3. Other examples can be found in the literature cited above. In the upper panels we show the caustic structure together with the source trajectory in the plane (θ_x, θ_y) . We place the lenses along the θ_x -axis at $\pm d/2$. In the lower panels we plot the lightcurves as functions of θ_x/θ_E , which for a uniformly moving source is related linearly to time.

In the interior neighborhood of a caustic, the magnification diverges as K/\sqrt{y} , where y is the angular distance perpendicular to the caustic, in units of the Einstein angle (Chang & Refsdal 1979, Kayser & Witt 1989). The flux factor K depends on the lens map through the length of the tangent vector to the caustic, $T = |T_\zeta|$, as $K = \sqrt{2/T}$. In the complex parameterization, the tangent vectors to the critical curve and caustic are (Witt 1990)

$$T_z = -2i \frac{\partial \alpha}{\partial z} \frac{\partial^2 \alpha}{\partial z^2}, \quad T_\zeta = T_z - \frac{\partial \alpha}{\partial z} \bar{T}_z. \quad (30)$$

Defining the Einstein time as usual $t_E = 2R_E/v$, and taking the angle to the normal as δ , the lightcurve near

the caustic crossing at $t = t_0$ is, in the interior side of the caustic,

$$F = \frac{F_0 K}{\sqrt{2 \cos \delta}} \sqrt{\frac{t_E}{\pm(t - t_0)}}, \quad (31)$$

with the + sign (− sign) when entering (exiting) the caustic. In pixel lensing F_0 is unknown (but see the next paragraph for a possibility to determine it). However, there are two caustic crossings, and if the timescales of the two are compared, the ratio of the geometric factors $K/\sqrt{\cos \delta}$ at each of the two caustic crossings can be measured. This may provide some insight into the exact parameters of individual events.

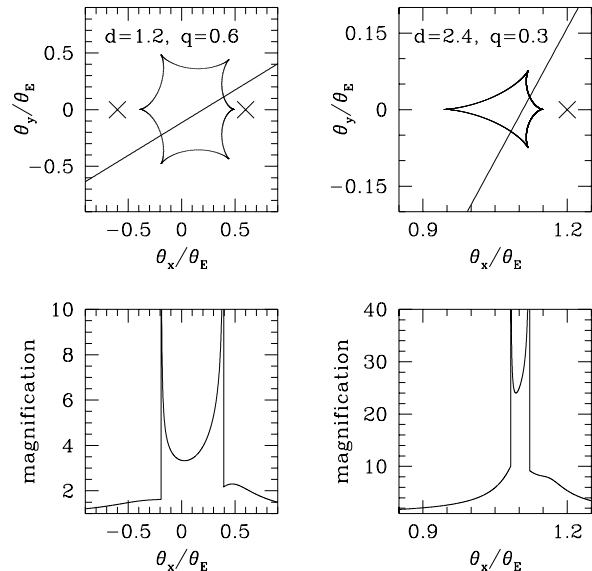


FIG 3.— Example source trajectories and lightcurves for caustic crossing events. The lenses are marked with crosses, the more massive on the right.

We may gain useful information by measuring the duration of the caustic crossing. This is the time over which the disk of the source star intersects the caustic, and is given simply by

$$t_{\text{cross}} = \frac{\theta_s}{\theta_E} \frac{t_E}{\cos \delta} = \frac{2Lx\theta_s}{v \cos \delta}. \quad (32)$$

For star–star lensing in a distant galaxy, $x \approx 1$, L is known, and v and $\cos \delta$ are taken from known distributions. This can give a handle on the angular size of the source star. Furthermore, if the caustic crossing is seen in multiple wavebands, the color(s) of the source star can be determined. This is possible because the magnification is the same in all wavebands, thus comparing the flux *increase* in two bands is the same as comparing the actual (unmeasured) source flux in those bands. With the color and the angular size, a rough estimate of the absolute flux F_0 can be derived. It may also be possible to image the surface of these extragalactic stars as the caustic passes over them, as has been done towards the SMC (Afonso et al. 1998; Albrow et al. 1999). However, this would require intense monitoring to cover the actual caustic crossing. It is not the purpose of this paper to discuss this possibility further.

The magnification during a caustic crossing is critically important to a calculation of the event rate. While the magnification of a point-like source is infinite, that of a real source is finite. Since only magnifications higher than a threshold magnification can be observed, it is crucial to determine the fraction $f(A > A_0)$ of caustic crossing events that exceed a fixed magnification A_0 . The rate of caustic crossings entering the caustic with magnification $A > A_0$ is then

$$\Gamma = f(A > A_0) \Gamma_0. \quad (33)$$

We now determine $f(A > A_0)$.

The maximum magnification of a finite source of angular radius θ_s is given by (Schneider & Weiß 1987)

$$A_{\max} = f_s K \sqrt{\frac{\theta_E}{\theta_s}}, \quad (34)$$

where f_s is a form factor depending on the luminosity profile of the source. For a uniform disk, $f_s = 1.39$, while a limb-darkened profile $\sim \sqrt{1 - r^2/R_s^2}$ gives $f_s = 1.47$ (Kayser & Witt 1989), thus we see that the profile is relatively unimportant for our purposes.

A_{\max} in eq. (34) is the highest magnification when the source crosses the caustic. It follows that the fraction of events that cross a given caustic with magnification $A > A_0$ is equal to the fraction of length of the caustic in which $K > K_0 \equiv A_0 \sqrt{\theta_s/\theta_E}/f_s$,

$$f(A > A_0) = \frac{w(K > K_0)}{w}. \quad (35)$$

Taking a distribution of mass ratios constant in q , we plot $w(K > K_0)$ as a function of d for several values of K_0 in figure 4.

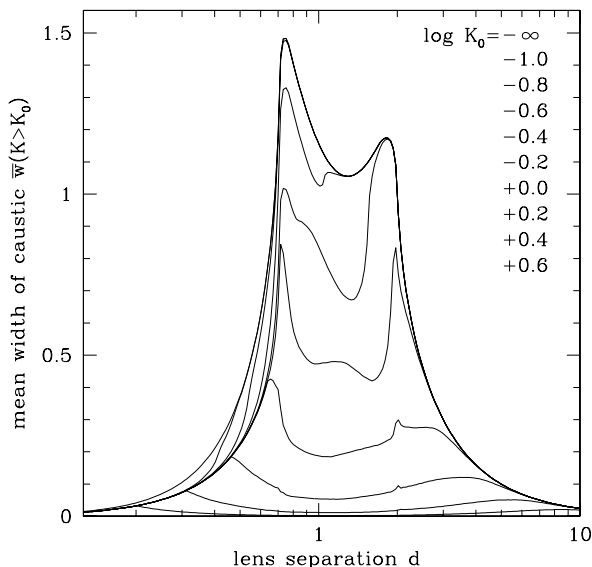


FIG 4.— Effective width of the caustic structure $w(K > K_0)$. We choose values equally spaced in $\log K_0$. The curves decrease in magnitude as K_0 increases.

7. EVENT RATE

We now compute the rate distribution of caustic crossing events. We let the velocity distribution of the source

and lens population be Maxwellian with characteristic velocity v_c . We denote the transverse velocity of the lens v_t , and the transverse velocity of the line-of-sight v_l . We denote the total mass of the lens M , and the apparent magnitude of the source m . We define the mass function $\xi(M) = dN/dM$ normalized to unity, and the luminosity function $\phi(m)$ normalized to the surface brightness. We denote the distribution in d as $\Pi(d) = 3/(20d \ln 10)$. The mean width of the caustic structure in Einstein units is w , and we choose a distribution constant in q .

We will compute the rate of caustic crossing events with respect to the time between caustic crossings t_C in two ways. First we will use the mean length of chords to determine this timescale, which is not correct event by event, but may be acceptable for a rate distribution. If we define the effective time between caustic crossings

$$t_{\langle C \rangle} = \frac{R_E \langle C \rangle}{v_t}, \quad (36)$$

where $\langle C \rangle = \langle C(d) \rangle$ is the length of the caustic chord averaged over the q distribution, we can write the rate distribution as

$$\frac{d\Gamma}{dt_{\langle C \rangle}} = 2Lv_c^2 \int dm \phi(m) \int dM \frac{\xi(M)}{M} \int_0^1 dx \rho'(x) \quad (37)$$

$$\int_{d_{\min}}^{\infty} dd \Pi(d) \omega^4 e^{-(\omega-\eta)^2} \tilde{I}_0(2\omega\eta) \frac{w(K > K_0)}{\langle C(d) \rangle}.$$

with d_{\min} given below, $\omega = R_E(x)\langle C(d) \rangle/(v_c t_{\langle C \rangle})$ and $\eta = v_l/v_c$. Also, $\tilde{I}_0(x) = I_0(x)e^{-x}$, where I_0 is a modified Bessel function of the second kind. We note that $\tilde{I}_0(x \gg 1) \approx 1/\sqrt{2\pi x}$ and $\tilde{I}_0(0) = 1$.

Secondly, we will use the actual caustic crossing timescale, at the cost of doing an exhaustive Monte Carlo of chord lengths. Here we define t_C as in eq. (36), except that now C is the actual chord length. The rate distribution is then

$$\frac{d\Gamma}{dt_C} = 2Lv_c^2 \int dm \phi(m) \int dM \frac{\xi(M)}{M} \int_0^1 dx \rho'(x) \quad (38)$$

$$\int_0^{\infty} dv v^3 e^{-(v-\eta)^2} \tilde{I}_0(2\eta v) w_{\text{eff}} \left(\frac{v_c t_C}{R_E} v, K > K_0 \right),$$

with $v = v_t/v_c$, w_{eff} being the effective width as a function of chord length,

$$w_{\text{eff}}(C, K_0) = \left\langle w \frac{dN}{dC}(K > K_0) \right\rangle_{\theta, q, d}, \quad (39)$$

w is the projected diameter given in eq. (29), and dN/dC is the probability distribution of chord lengths at a given θ, q, d , computed by Monte Carlo and normalized to unity at $K_0 = 0$. We illustrate the function w_{eff} for several values of K_0 in figure 5.

To fix the minimum flux factor K_0 , we adopt the convention that the signal to noise totaled throughout the approximate lightcurve eq. (31), be greater than $Q_0 = 7$. We assume that samples are taken daily, (except for the reference case of the Milky Way Bulge, monitored continuously). The lightcurve is truncated first by assuming the first sample is taken at one half day away from the

caustic crossing, and then by requiring that the stellar diameter is less than the length of the chord. We derive the signal to noise as follows. Assume that the telescope collects photons from a source of magnitude m at a rate $S_0 10^{-0.4m}$. An integration of t_{int} per observation is taken. The background galaxy light falling on the pixel has a magnitude μ . This gives a signal to noise per sample of $Q = \sqrt{S_0 t_{\text{int}}} 10^{-0.4(m-\mu/2)} (A-1)$, where we have only considered photon noise. Ground based microlensing surveys have achieved noise levels within a factor of two of the photon noise, and we expect space based surveys to approach the photon noise limit. Thus there is a simple relation between the minimum allowed $Q = Q_0$ and the minimum flux factor K_0 .

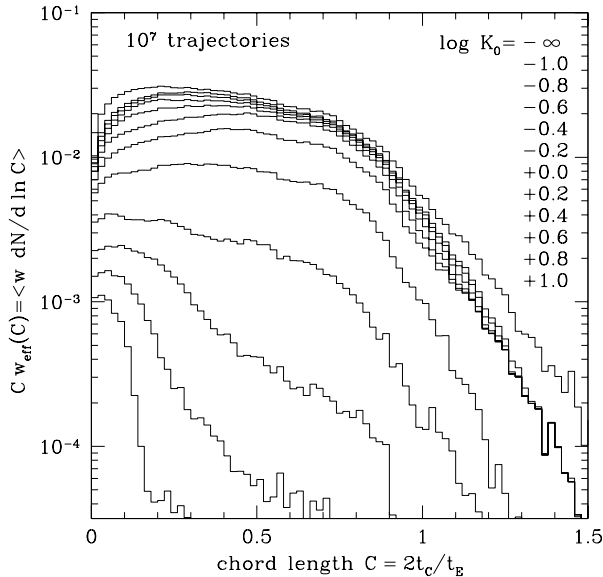


FIG 5.— Effective width for caustic crossing events. Ten million trajectories through caustic structures have been generated for various values of d , q , and θ , and the histograms appropriately weighted for several values of K_0 . The w_{eff} histograms have been multiplied by C for clarity.

The minimum d allowed is determined by fixing the period at its minimum, 10^{-3} yr, giving $d_{\text{min}} = 0.02(M/M_\odot)^{-1/6} B(x)^{-1}$. In practice, fixing $d_{\text{min}} = 0.1$ is fine, since d lower than this gives a very small cross section, and for the mass we are concerned with, it gives a minimum lens–source distance of 10 pc, which is negligible. In principle a maximum d can be determined by the binding of the binary, but it is never important observationally.

The density $\rho'(x)$ is the effective density of source–lens systems at separation x , and can be determined by integrating the source and lens positions along the line of sight through the target system. Assuming a radial density profile of stars $\rho(r)$ truncated at a radius R , we calculate the column density along a line of sight with impact parameter b ,

$$N = \int_{-\sqrt{R^2-b^2}}^{\sqrt{R^2-b^2}} \rho(\sqrt{b^2+s^2}) ds. \quad (40)$$

The density along the line of sight is used as a probability distribution for sources. Using $y = 1 - x$, and assuming $L \gg s$ (which furthermore implies that R_E only depends

on y and L and not on s), we find

$$\rho'(1-y) = \int_{-\sqrt{R^2-b^2}}^{\sqrt{R^2-b^2}-yL} \frac{1}{N} \rho(\sqrt{b^2+s^2}) \times \rho(\sqrt{b^2+s^2+2Lys+L^2y^2}) ds. \quad (41)$$

Finally, we comment on the rate of binary events with resolved sources. In this case there is no maximum x , as any caustic crossing event can be detected. Thus the integral over the luminosity function $\phi(m)$ is trivial. The remaining triple integral is simply multiplied by the number of monitored stars.

8. BACKGROUNDS AND BLENDING

In any microlensing survey, the issue of backgrounds is crucial. In considering binary microlensing events, the lightcurves are basically characterized by a double spike. Such events in isolation should be exceedingly rare. The most pernicious of backgrounds for single lens events is the mira variables (Crotts et al. 2000), which have a very long period, but as they are characterized by a single spike, we are unconcerned with them. However, if one of the two caustic crossings is missed, the characterization of the event as microlensing would be very difficult, and only possible with a very high signal to noise and/or long follow-up period.

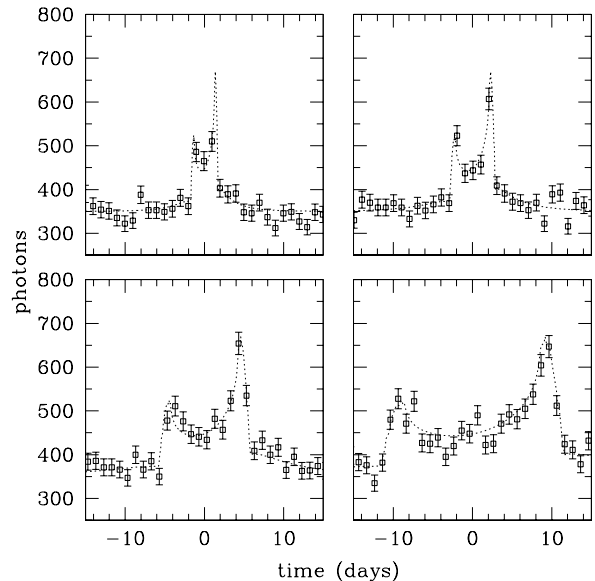


FIG 6.— Simulated lightcurves in the ACS. The binary system is the same as in the left panels of figure 3. We illustrate lightcurves where the time between caustic crossings is 3, 5, 10, and 20 days. The brightness is $27.5 \text{ mag pixel}^{-1}$, the source star has an apparent magnitude of 28.5 in I , and we have accounted for the ACS PSF. The dotted curves indicate the theoretical expectation, including finite source effects.

In uncovering variability, we must be concerned with the amount of blending of the lensed star’s light. We will now make a simple estimate of this quantity. We want to know first the typical magnitude of the lensed star. Studying a typical I -band luminosity function, such as that of Terndrup, Frogel & Whitford (1990), we see that the slope

at the highest fluxes is shallower than 0.4, meaning that the most light comes from the brightest stars. This means that the majority of detectable microlensing events will be microlensing of very bright stars. In fact, typically the rate of such events is expected to peak somewhere between the surface brightness fluctuation magnitude (which for the Terndrup et al. (1990) luminosity function is roughly $\overline{M}_I = -1.5$) and the tip of the red giant branch (at roughly $M_I = -3.5$). As a rough estimate for M87, if we assume the pixel scale of the Advanced Camera for Surveys (ACS) on the HST is $0.05''$, and a surface brightness of roughly $21 \text{ mag arcsec}^{-2}$ for most of the field of view, the pixel brightness is $27.5 \text{ mag pixel}^{-1}$, while the surface brightness fluctuation magnitude is roughly 29.5 for M87, meaning that each pixel has the light of roughly 6 SBF magnitude stars. Moreover, we assume a PSF where roughly 25% of the light of a star falls on the central pixel. This means that if we desire the pixel flux to double, the typical required magnification (for $M_I = -2.5$) is a factor of 12. In an 1800 second integration with the ACS at this surface brightness, roughly 350 photons are collected, so a 10σ excess requires only a 50% magnification of the pixel flux, or a microlensing magnification that is typically of order six.

In figure 6, we illustrate four representative lightcurves of a binary event in M87 observed by the HST ACS, sampling daily. In all cases the geometry is identical to the left panel of figure 3, but with four different timescales between caustic crossings of 3, 5, 10, and 20 days. With a timescale of three days, though the event is detected at a significant signal to noise, it is not convincingly a binary. With a timescale of five days or more, it seems more likely that binary events can be unambiguous.

Finite source size effects are not severe for the example lightcurves in figure 6. The star of magnitude $M_I = -2.5$ has a radius of roughly $65 R_\odot$ (Gould 1995), and for a solar mass lens system with $D_{ds} \approx 5 \text{ kpc}$, the star subtends roughly one seventh of the angular distance between caustics along its path. The dotted curves are the theoretical lightcurves, including finite source effects for a uniform surface brightness star, computed according to Gould & Gauchere (1997). According to eq. (34), the limiting counts should be roughly 475 on the left and 600 on the right. As shown, the full calculation is not quite that severe. That the lightcurves should not be seriously affected is also clear from the fact that the angular size of the star is small relative to the angular distance between the caustics. For the two longer events, it becomes possible to see the actual caustic crossing happening, though with one image a day the accuracy is poor. In principle, one could envision an alert system so that more frequent images are recorded during a suspected caustic crossing.

9. EXAMPLE MICROLENSING SURVEYS

We consider the case of star–star lensing in M87, a giant elliptical in the Virgo cluster at a distance of 15.8 Mpc. We take the radial profile of stars to be

$$\rho(r) = \rho_0 \left[1 + \left(\frac{r}{\text{kpc}} \right)^2 \right]^{-\alpha}, \quad (42)$$

with

$$\alpha = \max \left[1, 1 + 0.275 \log \left(\frac{r}{\text{kpc}} \right) \right], \quad (43)$$

and $\rho_0 = 3.76 M_\odot \text{ pc}^{-3}$, following Tsai (1993). We adopt the *I*-band luminosity function of Terndrup et al. (1990) adjusted to yield a surface brightness fluctuation magnitude of $\overline{M}_I = -1.5$, and a mass function $M\xi(M) \propto \exp(-.417 \ln M - 0.0886 \ln^2 M)$ with M in solar masses (Miller & Scalo 1979). The velocity dispersion is taken to be $v_c = 360 \text{ km s}^{-1}$. Typically, stellar radii are $\theta_s \sim 10^{-13}$, while the typical Einstein radii are of order $\theta_E \sim 2 \times 10^{-12}$ for solar mass lenses, a factor of twenty larger. We compute the rate of caustic crossing events observed in surveys using the ACS on the HST, and on a model NGST. We compare with the rate of single–lens events (Baltz & Silk 2000), requiring seven samples detected at 2σ , as Criteria A of Alcock et al. (2000b). We assume that the sensitivity of the ACS is 4.5 times that of the WFPC2 in the *I* band, meaning that one photon per second is collected from a star of magnitude $m_I = 25.77$, integrated over the entire PSF. We model the NGST as having seven times the efficiency of WFPC2, but with nine times as much collection area. These rates are plotted in the upper panels of figure 7. In a monitoring program of daily observations of M87 for a period of a month, the Advanced Camera for Surveys on HST would detect of order one caustic crossing event, and the NGST could detect of order one dozen caustic crossing events.

Microlensing in M31, the Andromeda Galaxy, has been searched for extensively using the pixel technique (Ansari et al. 1997, 1999; Melchior et al. 1998, 1999; Crofts and Tomaney 1996; Tomaney and Crofts 1996). We have computed the rate of caustic crossing events observed in the bulge of M31, assuming a CFHT–class telescope and using the bulge model of Kent (1989), with a velocity dispersion of $v_c = 220 \text{ km s}^{-1}$. The typical star has a radius $\theta_s \sim 2 \times 10^{-12}$, and the typical Einstein radius is $\theta_E \sim 4 \times 10^{-11}$, again a factor of 20 larger. The fiducial star has magnitude $m_I = 26.88$, giving one photon per second integrated over the PSF. Furthermore, we assume that the errors are twice the photon counting noise, as found by the AGAPE collaboration (Ansari et al. 1997). We again compare with the rate of single–lens events, and plot the results in figure 7. A CFHT survey of the bulge of M31 would detect on the order of one binary event per month of observations.

Finally we compare the rates of single–lens and caustic crossing events towards the bulge of the Milky Way. We take the simple bulge and disk model of Evans (1994), with no bar. These rates are plotted in the upper panel of figure 7. Note that typically 10^7 stars are monitored in the galactic bulge. We notice that our rates are comparable to the the results of the MACHO project monitoring of the galactic bulge (Alcock et al. 1997; 2000a). While we find that roughly 6% of events should exhibit caustic crossings in this case, the finite stellar radii remove a significant fraction of these events as the stellar radius becomes comparable to the distance between the caustics, and we find that roughly 2–3% of events will exhibit detectable caustic crossings.

We find that caustic crossing events typically make up 10%, and as much as 15%, of the total rate of stellar events

in pixel microlensing surveys, assuming that all stars are binaries. This is significantly higher than the relative rate in microlensing with resolved sources, typically 2-3%. Thus, the larger effective cross section is more important than the more severe finite source effects.

These estimates all assume only self-lensing in the target galaxy. Of course there is the possibility that lenses in the halo of the Milky Way could contribute. Unless there is a significant population of halo lenses, the rate for stellar lenses in the Milky Way would be substantially smaller than the self-lensing rate in the target galaxy, since the scale height of the disk is much smaller than the size of the spheroids of the target galaxies.

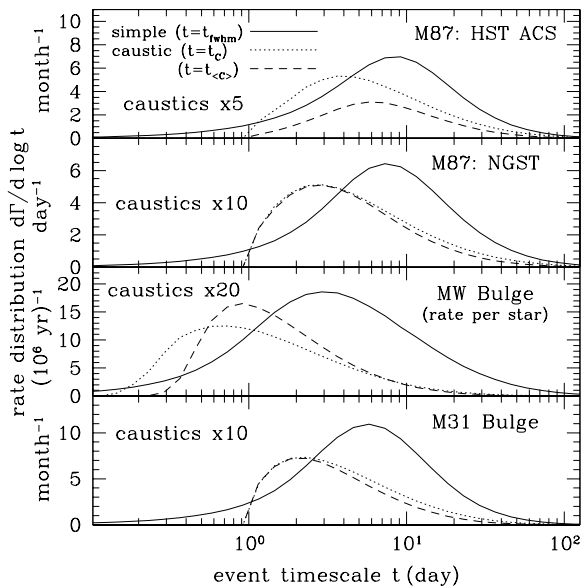


FIG 7.— Rate of microlensing events. In all cases the solid lines indicate the rate of single-lens events as a function of the full-width at half maximum timescale t_{fwhm} , the dotted lines indicate the rate of caustic crossing events as a function of crossing time t_C , and the dashed lines indicate the caustic crossing rate using the mean crossing time $t_{\langle C \rangle}$. *Top panel:* M87 events using the Advanced Camera for Surveys on HST. *Second panel:* M87 events using the NGST. *Third panel:* Milky Way bulge events for resolved stars. This rate is quoted per monitored star. *Bottom panel:* Events in the bulge of M31. We use the improved peak threshold trigger for single-lens events in M31 and M87. A Miller-Scalo mass function is assumed in all systems.

From figure 7 we see that the time between caustic crossings is typically of order several days. Sampling daily would allow a sizeable fraction of the lightcurves to be well-measured. We also see that for long timescale events, the timescale $t_{\langle C \rangle}$ gives a very good approximation to the true rate (using t_C), but for the shorter events, it is less accurate. We notice that the agreement between the two is excellent for the NGST and for the M31 bulge. In these cases, the required magnification is quite modest, of order a factor of two for a star with the surface brightness fluctuation magnitude. The ACS requires significantly higher magnifications, spoiling the excellent agreement between the rate with respect to the two timescales t_C and $t_{\langle C \rangle}$. For the Milky Way Bulge, the agreement between the two

timescales is quite good, though the (quite broad) peaks disagree by a factor of about two in timescale. We thus find that the timescale $t_{\langle C \rangle}$ provides a surprisingly good estimate of the rate of events with respect to the time between caustic crossings.

Finally, we comment that with daily sampling, the fine details of the caustic crossing will not be well covered. If we choose a finer sampling scheme, with the same telescope resources, the expected number of events will be much smaller. We feel that it is important first to identify binary lensing events. If this is shown to be possible, then more sophisticated sampling strategies should of course be considered.

10. EXTRAGALACTIC PLANETS

As an aside, we apply the previous analysis to a pixel microlensing search of extragalactic planets.

Discovering planets outside our own solar system has been an important scientific goal for many years. The planets that have been discovered so far were all found by detecting the wobble of the star that they orbit. The first detection was of a planet approximately the mass of Earth, in orbit around a pulsar (Wolszczan & Frail 1992; Wolszczan 1994). More recently, planets have been detected around main sequence stars (see Marcy, Cochran & Mayor 2000 for a review). We would like to extend the range of planetary searches to distant galaxies. Gott (1981) was the first to point out that gravitational lensing might be used to detect low-mass objects in distant galaxies. Here we make another suggestion: pixel microlensing surveys may be able to detect Jupiter-mass planets as far away as the Virgo cluster, by capitalizing on the unique nature of binary microlensing events.

Previous work has shown that planets might be detected in microlensing events in the bulge of the Milky Way galaxy, or in the Small and Large Magellanic Clouds, which are small galaxies in orbit around the Milky Way (Mao & Paczyński 1991, Gould A. & Loeb, A. 1992, Griest, K. & Safizadeh, N. 1998). Stars in the bulge and in the Magellanic clouds can be resolved easily, and surveys routinely monitor of order ten million stars for microlensing events. Evidence for a planet orbiting a binary star system in the Milky Way bulge has recently been claimed in a joint publication of the MPS and GMAN collaborations (Bennett et al. 1999), although the data can also be interpreted as a rotating binary system without a planet (Albrow et al. 2000).

A solar-type planetary system can be described to first approximation as a binary object, consisting primarily (in mass) of the Sun and the planet Jupiter. In such systems q is very small, for example $q \approx 10^{-3}$ for the Sun and Jupiter. In figure 8, we show two example lightcurves of microlensing events, together with the trajectories of the source stars relative to the caustic curves. In both cases the star has a companion one one-thousandth as massive, like the Sun-Jupiter system.

We have calculated the rate of planetary events observing M31 with a telescope like the Canada-France-Hawaii telescope (CFHT) on Mauna Kea. We assume that every star has a companion that is one one-thousandth as massive, just like the Sun and Jupiter. Furthermore, we assume, as is true for known binary stars, that the distribution of orbital periods is such that ten percent of such

systems lie in each decade of period, from a third of a day to ten million years. This gives a 10% probability that a star has a companion between one and five AU, in rough agreement with observational findings (Marcy, Cochran & Mayor 2000). With a long-term monitoring program observing four times daily (using the necessary global network of telescopes), and relaxing the threshold to be three sigma in the two images appearing inside the caustic, we expect about one caustic crossing planetary event every two years. This neglects other types of microlensing anomalies, such as those discussed by Covone, de Ritis & Marino (1999).

To increase the chances to detect planetary systems in distant galaxies, we require a space telescope such as the proposed Next Generation Space Telescope, to be launched around 2009. This will be a large (about 7 meters in diameter) infrared telescope at a Lagrange point of the Earth-Sun system, and it will be more than ten times as sensitive as the Hubble Space Telescope.

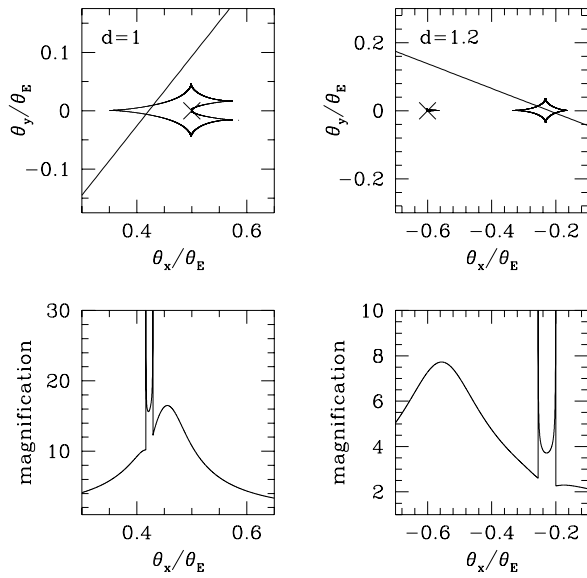


FIG 8.— Microlensing events due to a planetary system. We illustrate the trajectory of a source star over the caustic curves of a lens star and its planet. We then illustrate the observed magnification of the source star along its trajectory. The cross indicates the star's position, whereas the planet lies off the plots at -0.5 and 0.6 , respectively. The plots are in units of the Einstein angle θ_E , which is the characteristic angular scale of a microlensing event. Also shown is the star-planet separation d in units of θ_E .

We have calculated the rate of events we might detect with the NGST observing the giant elliptical galaxy M87 in the Virgo cluster, at a distance of 15.8 Mpc. With the same assumptions as the M31 calculation, we find that an NGST survey of three month's duration, taking four images each day, should be able to detect of order four planetary systems. We find that such a survey is most sensitive to events where the separation between caustic crossings is about five days. An alert system for microlensing events would allow more frequent measurements of the light curve during the caustic crossings, with the possibility of determining the orbital parameters of the planetary system.

Our results for the rate of caustic crossing planetary events indicate that the rates are probably too small for this technique to be a feasible method of detecting extragalactic planets. We have made overly generous assumptions, and still the detection probabilities are marginal.

11. CONCLUSIONS

We have found that caustic crossing binary events should typically make up 10%, and as much as 15%, of the total rate of events in pixel microlensing surveys. This is significantly higher than the relative rate in microlensing with resolved stars, which is typically 2-3%. The enhancement is due to the larger magnification of caustic crossing events with respect to single-lens events. The suppression in the count rate expected from finite-source effects is not large enough to win over the enhancement from larger regions of high magnification.

In examples of pixel lensing surveys, we find that on the order of one binary event per month of observation should be observable in a CFHT survey of the bulge of M31. Also of the order of one caustic crossing event per month of daily observations of M87 should be detectable with the Advanced Camera for Surveys on HST. The latter rate would increase to of order one dozen caustic crossing events per month with the NGST. Searches for extragalactic planets with the microlensing technique discussed in this paper do not seem particularly promising.

We would like to thank the referee for constructive comments that have added much to the original manuscript, and for making us aware of a simplification of eq. (4). E. B. thanks P. Podsiadlowski for productive conversations concerning binary star systems. We thank J. Silk for useful comments and hospitality at Oxford University, where this research was begun. E. B. was supported in part by grants from NASA and DOE.

REFERENCES

- Afonso, C. et al. 1998, *A&A*, 337, L17
Afonso, C. et al. 2000, *ApJ*, 532, 340
Albrow, M. D. et al. 1995, *ApJ*, 509, 687
— 1998, *ApJ*, 509, 687
— 1999, *ApJ*, 512, 672
— 2000, *ApJ*, 534, 894
Alcock, C. et al. 1995, *ApJ*, 449, 28
— 1997, *ApJ*, 479, 119
— 1999, *ApJS*, 124, 171
— 2000a, *ApJ*, 541, 270
— 2000b, *ApJ*, 542, 281
Ansari, R. et al. 1997, *A&A*, 324, 843
— 1999, *A&A*, 344, L49
Baillon, P., Bouquet, A., Giraud-Héraud, Y., & Kaplan, J. 1993, *A&A*, 277, 1
Baltz, E. A. & Silk, J. 2000, *ApJ*, 530, 578
Bennett, D. et al. 1999, *Nature*, 402, 57
Chang, K. & Refsdal, S. 1979, *Nature*, 282, 561
Covone, G., de Ritis, R. & Marino, A. A. 1999, *astro-ph/9903285*
Crotts, A. P. S. 1992, *ApJ*, 399, L43
Crotts, A. P. S. & Tomaney, A. 1996, *ApJ*, 473, 87
Crotts, A. P. S., Uglesich, R., Gould, A., Gyuk, G., Sackett, P., Kuijken, K., Sutherland, W. & Widrow, L. 2000, *astro-ph/0006282*
di Stefano, R. & Perna, R. 1997, *ApJ*, 488, 55
Duquenois, A. & Mayor, M. 1991, *A&A*, 248, 485
Einstein, A. 1936, *Science*, 84, 506

- Erdl, H. & Schneider, P. 1993, *A&A*, 268, 453
Evans, N. W. 1994, *ApJ*, 437, L31
Gott, R. J. 1981, *ApJ*, 243, 140
Gould, A. 1995, *ApJ*, 455, 44
Gould, A. & Gauchere, C. 1997, *ApJ*, 477, 580
Gould, A. & Loeb, A. 1992, *ApJ*, 396, 104
Griest, K. 1991, *ApJ*, 366, 412
Griest, K. & Safizadeh, N. 1998, *ApJ*, 500, 37
Han, C., Park, S.-H., & Lee, Y.-S. 2000, *MNRAS*, 314, 59
Kayser, R. & Witt, H. J. 1989, *A&A*, 221, 1
Kent, S. M. 1989, *AJ*, 97, 1614
Mao, S. & di Stefano, R. 1995, *ApJ*, 440, 22
Mao, S. & Paczyński, B. 1991, *ApJ*, 374, L37
Marcy, G. W., Cochran, W. D. & Mayor, M. 2000, in *Protostars and Planets IV*, ed. V. Mannings, A. P. Boss & S. Russell (Tucson: University of Arizona Press), in press
Mazeh, T., Goldberg, D., Duquennoy, A. & Mayor, M. 1992, *ApJ*, 401, 265
Melchior, A.-L. et al. 1998, *A&A*, 339, 658
—, 1999, *A&AS*, 134, 377
Miller, G. E. & Scalo, J. M. 1979, *ApJS*, 41, 513
Paczynski, B. 1986, *ApJ*, 304, 1
Patience, J., Ghez, A. M., Reid, I. N., Weinberger, A. J., Matthews, K. 1998, *AJ*, 115, 1972
Rhie, S. H. & Bennett, D. P. 1999, *astro-ph/9912050*
Schneider, P. & Weiß, A. 1986, *A&A*, 164, 237
Schneider, P. & Weiß, A. 1987, *A&A*, 171, 49
Terndrup, D. M., Frogel, J. A., & Whitford, A. E. 1990, *ApJ*, 357, 453
Tomaney, A. & Crotts, A.P.S. 1996, *AJ*, 112, 2872
Trimble, V. 1990, *MNRAS*, 242, 79
Tsai, J. C. 1993, *ApJ*, 413, L59
Udalski, A. et al. 1994, *ApJ*, 436, L103
Udalski, A., Żebruń, K., Szymański, M., Kubiak, M., Pietrzyński, G., Soszyński, I., & Woźniak, P. 2000, *astro-ph/0002418*
Witt, H. J. 1990, *A&A*, 236, 311
Wolszczan, A. & Frail, D. A. 1992, *Nature*, 355, 145
Wolszczan, A. 1994, *Science*, 264, 538